With respect to the indicated comments, we give you the answers. The manuscript changes in red text and the previous manuscript in green text.

1) Answers for Referee #2:

Table 1

1) Your comment: *In Table 1- Please insert LAT /LONG cordinate of each station.*

Answer: We agree with your comment. Therefore, we have done correction as follow:

Now:

Table 1. a) Events analyzed in this study: Peñamiller Earthquake Sequence (PES); b) Station location .

a)

Event No.	UTC Date (yyyy/mm/dd)	Number Records	Station Name
1	2011/01/30	3	EXT1, PIL1, HIG1
2	2011/01/30	3	EXT1, PIL1, HIG1
3	2011/02/07	3	EXT1, PIL1, HIG1
4	2011/02/07	3	EXT1, PIL1, HIG1
5	2011/02/08	3	EXT1, PIL1, HIG1
6	2011/03/01	3	EXT1, PIL1, HIG2
7	2011/03/01	3	EXT1, PIL1, HIG2
8	2011/03/26	3	EXT1, PEN2, HIG2
		24	

b)

Station Name	Location		
	Community	Lat. (°N)	Long. (°W)
EXT1	Extoraz	21.036	-99.777
PIL1	Pilon	21.065	-99.775
HIG1	Higuerillas	20.920	-99.763
PEN2	Peñamiller Center	21.054	-99.814
HIG2	Higuerillas	20.921	-99.770

Before:

Table 1. Events analyzed in this study: Peñamiller Earthquake Sequence (PES).

Event No.	UTC Date (yyyy/mm/dd)	Number Records	Station Name
1	2011/01/30	3	EXT1, PIL1, HIG1
2	2011/01/30	3	EXT1, PIL1, HIG1
3	2011/02/07	3	EXT1, PIL1, HIG1
4	2011/02/07	3	EXT1, PIL1, HIG1
5	2011/02/08	3	EXT1, PIL1, HIG1
6	2011/03/01	3	EXT1, PIL1, HIG2
7	2011/03/01	3	EXT1, PIL1, HIG2
8	2011/03/26	3	EXT1, PEN2, HIG2
		24	

2) Your comment:*In Table 4 and Table 6 the averages of DIP an rake direction and sigmas has been onbtained with rigorous circular statistics metodolgies? Please check because some difference may exist in the contrary, because the angular or directional data a simple arithmetic average is not acceptable in some case are affected the final values.*

Answer: We agree with your comment. However, the average values shown in Table 4 and 6 are not essential in the discussion of this article, therefore we have decided that these can be retired of the article.

Now:

Table 4. Earthquake source parameters of best fit solutions from the Peñamiller sequence.

Event	UTC Date	Origin time	Location			Magnitude	Strike	Dip	Rake	Number
		UTC Hour	Lat.	Long.	H	Mw	ϕ	δ	λ	
No.	(yyyy/mm/dd)	(hh:mm:ss)	(°N)	(°W)	(km)		(°)	(°)	(°)	Records
1	2011/01/30	17:54:22.50	21.034	-99.756	5.7	2.1	154	61	-116	3
2	2011/01/30	17:54:41.70	21.034	-99.756	5.6	3.0	108	45	-149	3
3	2011/02/07	00:16:34.00	21.039	-99.754	5.5	2.9	41	57	-162	3
4	2011/02/07	09:42:54.50	21.024	-99.725	2.0	2.5	268	86	-5	3
5	2011/02/08	19:53:48.60	21.039	-99.752	5.6	3.5	174	77	-85	3
6	2011/03/01	12:59:40.70	21.031	-99.759	6.1	3.2	85	67	-152	3
7	2011/03/01	13:11:28.10	21.033	-99.758	6.1	2.7	133	64	-143	3
8	2011/03/26	01:42:17.40	21.015	-99.806	4.3	2.9	124	34	-14	3

Table 6. Earthquake source parameters and values of the maximum (σ_1) and minimum (σ_3) compressive principal stresses axes from the PES.

Event	UTC Date	Time origin	Magnitude	Strike	Dip	Rake	σ_1 (P)		σ_3 (T)	
		UTC Hour	Mw	ϕ	δ	λ	Azimuth	Plunge	Azimuth	Plunge
No.	(yyyy/mm/dd)	(hh:mm:ss)		(°)	(°)	(°)	(°)	(°)	(°)	(°)
1	2011/01/30	17:54:22.50	2.1	154	61	-116	19	63	263	13
2	2011/01/30	17:54:41.70	3.0	108	45	-149	310	50	57	15
3	2011/02/07	00:16:34.00	2.9	41	57	-162	257	35	355	12
4	2011/02/07	09:42:54.50	2.5	268	86	-5	223	7	313	2
5	2011/02/08	19:53:48.60	3.5	174	77	-85	90	58	261	32
6	2011/03/01	12:59:40.70	3.2	85	67	-152	305	35	214	2
7	2011/03/01	13:11:28.10	2.7	133	64	-143	352	44	257	5
8	2011/03/26	01:42:17.40	2.9	124	34	-14	104	44	343	29

Before:

Table 4. Earthquake source parameters of best fit solutions from the Peñamiller sequence.

Event No.	UTC Date (yyyy/mm/dd)	Origin time UTC Hour (hh:mm:ss)	Location Lat. (°N)	Long. (°W)	H (km)	Magnitude Mw	Strike ϕ (°)	Dip δ (°)	Rake λ (°)	Number Records
1	2011/01/30	17:54:22.50	21.034	-99.756	5.7	2.1	154	61	-116	3
2	2011/01/30	17:54:41.70	21.034	-99.756	5.6	3.0	108	45	-149	3
3	2011/02/07	00:16:34.00	21.039	-99.754	5.5	2.9	41	57	-162	3
4	2011/02/07	09:42:54.50	21.024	-99.725	2.0	2.5	268	86	-5	3
5	2011/02/08	19:53:48.60	21.039	-99.752	5.6	3.5	174	77	-85	3
6	2011/03/01	12:59:40.70	21.031	-99.759	6.1	3.2	85	67	-152	3
7	2011/03/01	13:11:28.10	21.033	-99.758	6.1	2.7	133	64	-143	3
8	2011/03/26	01:42:17.40	21.015	-99.806	4.3	2.9	124	34	-14	3
						Averages	136	61	-103	

Table 6. Earthquake source parameters and values of the maximum (σ_1) and minimum (σ_3) compressive principal stresses axes from the PES.

Event No.	UTC Date (yyyy/mm/dd)	Time origin UTC Hour (hh:mm:ss)	Magnitude Mw	Strike ϕ (°)	Dip δ (°)	Rake λ (°)	σ_1 (P) Azimuth (°)	Plunge (°)	σ_3 (T) Azimuth (°)	Plunge (°)
1	2011/01/30	17:54:22.50	2.1	154	61	-116	19	63	263	13
2	2011/01/30	17:54:41.70	3.0	108	45	-149	310	50	57	15
3	2011/02/07	00:16:34.00	2.9	41	57	-162	257	35	355	12
4	2011/02/07	09:42:54.50	2.5	268	86	-5	223	7	313	2
5	2011/02/08	19:53:48.60	3.5	174	77	-85	90	58	261	32
6	2011/03/01	12:59:40.70	3.2	85	67	-152	305	35	214	2
7	2011/03/01	13:11:28.10	2.7	133	64	-143	352	44	257	5
8	2011/03/26	01:42:17.40	2.9	124	34	-14	104	44	343	29
			Averages	136	61	-103	208	42	258	14

3) ***Your comment:*** *In Table 7 should be restructured because in this form isn't enough clear for the readers.*

Answer: We agree with your comment. Therefore, we have done correction as follow:

Now:

Table 7. Amplitude of peak ground acceleration with respect to hypocentral distance from all events in each station.

		Event No.[Mw]							
		1 [2.1]	2 [3.0]	3 [2.9]	4 [2.5]	5 [3.5]	6 [3.2]	7 [2.7]	8 [2.9]
		Peak Ground Acceleration, PGA (cm/s^2) / Hypocentral distance R_h (km)							
Station	EXT1	4.66 / 6.11	27.23 / 6.02	9.28 / 6.01	8.26 / 5.93	93.63 / 6.19	36.24 / 6.41	7.82 / 6.42	8.12 / 5.74
	PIL1	4.95 / 6.95	30.40 / 6.86	5.58 / 6.59	4.42 / 7.19	83.12 / 6.74	16.81 / 7.36	14.75 / 7.28	-
	HIG1	0.69 / 13.92	1.91 / 13.88	0.50 / 14.36	0.52 / 12.39	3.44 / 14.41	-	-	-
	HIG2	-	-	-	-	-	1.51 / 13.68	0.38 / 13.89	1.18 / 11.87
	PEN2	-	-	-	-	-	-	-	4.91 / 6.14

PGA is root mean square of the horizontal components.

Before:

Table 7. Amplitude of peak ground acceleration with respect to hypocentral distance from all events in each station.

	Peak Ground Acceleration, PGA (cm/s^2) / Hypocentral distance R_h (km)							
Station /Event No.[Mw]	1 [2.1]	2 [3.0]	3 [2.9]	4 [2.5]	5 [3.5]	6 [3.2]	7 [2.7]	8 [2.9]
EXT1	4.66 / 6.11	27.23 / 6.02 /	9.28 / 6.01	8.26 / 5.93	93.63 / 6.19	36.24 / 6.41	7.82 / 6.42	8.12 / 5.74
PIL1	4.95 / 6.95	30.40 / 6.86 /	5.58 / 6.59	4.42 / 7.19	83.12 / 6.74	16.81 / 7.36	14.75 / 7.28	-
HIG1	0.69 / 13.92	1.91 / 13.88 /	0.50 / 14.36	0.52 / 12.39	3.44 / 14.41	-	-	-
HIG2	-	-	-	-	-	1.51 / 13.68	0.38 / 13.89	1.18 / 11.87
PEN2	-	-	-	-	-	-	-	4.91 / 6.14

PGA is root mean square of the horizontal components.

2) Corrected Paper

Seismicity at the northeast edge of the Mexican Volcanic Belt (MVB) and activation of an undocumented fault: the Peñamiller earthquake sequence of 2010-2011, Queretaro, Mexico

A. Clemente-Chavez[1], A. Figueroa-Soto[2], F. R. Zúñiga[2], M. Arroyo[1], M. Montiel[1] and O. Chavez[1].

[1]División de Investigación y Posgrado, Facultad de Ingeniería, Universidad Autónoma de Querétaro, Centro Universitario, Cerro de las Campanas s/n, Querétaro, Querétaro, C.P. 76010, México

[2]Centro de Geociencias (CGEO), Juriquilla, UNAM, P.O. Box 1-742, Querétaro, Querétaro, C.P. 76001, México

Correspondence to: A. Clemente-Chavez (aclemente09@alumnos.uaq.mx)

Abstract

The town of Peñamiller, in the state of Queretaro, Mexico is located at the northeast border of the seismogenic zone known as the Mexican Volcanic Belt (MVB), which transects the central part of Mexico with an east-west orientation. In this town, a sequence of small earthquakes occurred during the end of 2010 and beginning of 2011. Seismicity in the continental regimen of central Mexico is not too frequent, however, it is known that there are precedents of large earthquakes (Mw magnitude greater than 6.0) occurring in this zone. Three large earthquakes have occurred in the past 100 years: the 19 November 1912 (M_S7.0), the January 3 1920 (M_S 6.4) and 29 June 1935 (M_S 6.9). Prior to the instrumental period, the earthquake of 11 February 11 1875, which took place near the city of Guadalajara caused widespread damage.The purpose of this article is to contribute to the available seismic information of this region. This will help advance our understanding of the tectonic situation of the central Mexico and the MVB region.

Twenty-four shallow earthquakes of the Peñamiller, seismic sequence of 2011 were recorded by a temporary accelerograph network installed by the Universidad Autonoma de Queretaro (UAQ). The data were analysed in order to determine the source locations and to estimate the source parameters. The study was carried out through an inversion process and by spectral analysis. The results show that the largest earthquake occurred on February 8, 2011 at 19:53:48.6 UTC, had a moment magnitude Mw = 3.5, and was located at latitude 21.039° and longitude -99.752°, at a depth of 5.6 km. This location is less than 7 km away in a south-east direction from downtown Peñamiller. The focal mechanisms are mostly normal faults with small lateral components. These focal mechanisms are consistent with the extensional regimen of the southern extension of the Basin and Range (BR) province. The source area of the largest event was estimated to have a radius of 0.5 km, which corresponds to a normal fault with azimuth of 174° and an almost pure dip slip. Peak Ground Acceleration (PGA) was close to 100 cm s^{-2} in the horizontal direction. Shallow earthquakes induced by crustal faulting present a potential seismic risk and hazard within the MVB considering the population growth. Thus, the necessity to enrich seismic information in this zone is very important, since the risk at most urban sites in the region might even be greater than that posed by subduction earthquakes.

1 Introduction

The town of Peñamiller, in the Mexican state of Queretaro, is located at the northeast border of the seismogenic zone known as the Mexican Volcanic Belt (MVB), which extends through a central region of Mexico with east-west orientation, between the geographical coordinates 19° and 22° north latitude and 96° and 106° west longitude. The MVB is mostly a calc-alkaline volcanic arc which was formed as a result of subduction of the Rivera and Cocos plates underneath the North American plate (Suter, 1991).

The regional tectonic situation of the MVB is shown in Fig. 1. The central zone of the MVB includes several fault systems such as: Chapala-Tula (CTFS) (Johnson and Harrison, 1990); Morelia-Acambay (MAFS) (Martínez-Reyes and Nieto-Samaniego, 1990; Pasquaré et al., 1988); and Bajío (BFS) (Nieto-Samaniego et al., 1999; Alaniz-Álvarez and Nieto-Samaniego, 2005). This arc-parallel fault zone, and the volcanic arc itself, are superposed on a nearly perpendicular preexisting stress and deformation province, which may correspond to the extension of the Basin and Range (BR) into Mexico (Suter, 1991). The BR province

comprises north-northwest to north-northeast-striking normal faults, some of these faults are grouped in the Taxco-San Miguel Allende Fault Systems (TSMFS) (Demant, 1978; Pasquaré et al., 1987; Nixon et al., 1987). The orientation of major faults in the TSMFS zone was identified through satellite and aerial imagery analyzed by Aguirre-Díaz et al. (2005).

The western zone of the MVB includes several fault systems such as: Chapala (CHFS) defined as two half-graben of opposite convergence (Urrutia-Fucugauchi and Rosas-Elguera, 1994; Rosas-Elguera and Urrutia-Fucugauchi, 1998); Tepic-Zacoalco (TZFS), Colima (CFS) and Chapala (CHFS), intersecting at a triple junction to the south of Guadalajara (Demant, 1981).

The eastern zone of the MVB includes fault systems such as: Pera-Tenango (PTFS) with (García-Palomo et al., 2000; Ferrari et al., 2003); Aljibes (ALFS) and Mezquital (MZFS) with east-west orientations (Suter et al., 2001).

The stress state of the MVB zone has been inferred largely by major structures such as alignments of faults, shield volcanoes, dikes and elongations (e.g. Suter et al., 1995), mainly due to lack of seismic information because low frequency of seismic occurrence (Zúñiga et al., 2003). An example of the activity of this system was provided by the seismic sequence of Sanfandila, Queretaro, in 1998, reported by Zúñiga et al. (2003).

The historical seismicity in the MVB area shows that large earthquakes (see Fig. 1) can occur at depths less than 20 km (e.g. Singh et al., 1984; Suter et al., 1996; Zúñiga et al., 2003) with diverse fault styles. However, the most common mechanism type is extensional with north-south fault displacement (Zúñiga et al., 2003). In general, the MVB regional tectonics is characterized as extensional type with north-south fault displacements (Suter et al., 2001), although other orientations have been shown in some central parts of Mexico (Suter et al., 1995; Alaniz -Alvarez et al., 1998; Zúñiga et al., 2003).

Examples of similar documented events in other parts of the world where the seismic activity is too low are given in Polonia et al. (2012), Vipin et al. (2009) and Del Gaudio et al. (2009). In this study we present a detailed analysis of the seismic source parameters of events of the Peñamiller sequence, monitored during the first three months of 2011.

1.1 The Peñamiller seismic sequence

The sequence of small earthquakes (Mw <4.0) analyzed here took place at the end of 2010 and beginning of 2011. Peñamiller is located between the geographical coordinates 20°57' and 21°14' north latitude and 99°42' and 100°02' west longitude, in the foothills of the Sierra Gorda, about 80 km northeast of the City of Queretaro. As a result of reports of earthquakes that caused consternation in the local communities, a small seismic network consisting of three accelerographs was temporarily installed by the UAQ. The first part of the study consisted of identifying the origin of the activity and estimating the seismic source parameters, in order to analyze and associate its occurrence with the regional tectonic regime of the MVB.

Additionally, this paper also presents other information useful for hazard studies such as PGA. This information has not previously been reported for local earthquakes in the northeastern region of the MVB, and will help to contrast the vulnerability of population in the region to local seismic hazard sources to the vulnerability due to the occurrence of large regional events such as the large subduction earthquakes which occurr in the Pacific Coast. All results are presented and discussed in detail below.

2 Data analysis

A total of 24 accelerograms from 8 events were analyzed for the characterization of the Peñamiller Earthquake Sequence (PES), see Table 1. The three seismic stations were installed near the town of Peñamiller, at distances from 4 to 16 km. No other stations from the national network were available at suitable distances for recording these events. In two of the stations Etna accelerographs were installed, whereas a K2 model was employed in the third station (both models are Kinemetrics line). The station locations were chosen based on intensity reports from the local population, the safety of equipment and the need to provide good azimuthal coverage. The stations were located at three communities, whose names were associated with each station: Extoraz (EXT1), Pilon (PIL1, later renamed as PEN2 at Peñamiller Town Center, when it was relocated) and Higuerillas (HIG1, later renamed as HIG2, when it was relocated). All stations are shown in Fig. 2.

2.1 Seismic location

The SEISAN software package (Havskov and Ottemoller, 2000) was used to locate the events, using the crustal velocity model shown in Table 2, which was a modified version of Zúñiga et al. (2003) following the model determined by Fuentes (1997). It was deduced from surface wave dispersion of Rayleigh waves across the MVB. The location results are shown in Table 3, which show that the events occurred at depths around 5 km and distances between 4 to 10 km from downtown Peñamiller in a southeast direction (see Fig. 3). Table 3 also shows small error values (less than 1.34 km and rms of 0.07s).

2.2 Source parameters

To estimate the source parameters of the events, ISOLA software (Sokos and Zahradnik, 2008) was used. This program employs waveform modeling (inversion) to determine the focal mechanism and the scalar seismic moment. ISOLA software is based on a multiple point-source representation and an iterative deconvolution method, similar to Kikuchi and Kanamori (1991) for teleseismic records, but here the full wavefield is considered, and Green's functions are calculated by the discrete wavenumber method of Bouchon (1981). Thus the method is applicable for regional and local events (Sokos and Zahradnik, 2008). The code transforms velocity into displacement, inverts the displacement, and provides synthetic displacement (Sokos and Zahradnik, 2008).

An inversion on eight events of Table 3 was performed. The results are shown in Table 4 and Fig. 3, where the largest earthquake analyzed had Mw = 3.5 and occurred on February 8 at 19:53:48.6 UTC, although it is possible that a larger event (Mw > 3.5) in the episode was missed because it occurred before the network was installed.

The lineaments of the geomorphological features in the vicinity of the epicentral area and all the focal mechanisms are shown in Fig. 3a, where there is a strike tendency in the southeast direction; this can be seen from the average values shown in Table 4. The fault associated to the largest shock has a strike of 174°, dip of 77° and rake of - 85°. In general, the results of the focal mechanisms are mostly normal (see Fig. 3a and discussion) with a small lateral component. This is consistent with the main trend of the southern extension of the BR (Henry and Aranda-Gómez, 1992; Suter, 1991).

The waveform modeling was done on the P wave phase in its three components EW, NS and V. A band-pass filter between 0.35 Hz to 4.5 Hz was applied to obtain displacement, since it

was desired that the focal parameters be retrieved from the low frequency signal of the records, eliminating the noise produced by high frequency scatter waves and unknown crustal structure details (Zúñiga et al., 2003).

Fig. 4 shows the observed P wave and best fitting synthetic records obtained after the inversion for the largest event.

2.2.1 Spectral analysis

A spectral analysis on the seismic signal from the largest earthquake of the sequence was subsequently performed. This was done for P-wave and S-wave phases separately (see Fig. 5 and 6). In order to do this, the acceleration was twice-integrated to obtain displacement. The velocity signal is shown in Fig. 5, where it can be seen that a special baseline correction was not needed. The purpose of this analysis was to estimate some source parameters that the inversion procedure does not take into account such as fault radius (a), stress drop ($\Delta\sigma$) as well as the moment magnitude (Mw). A correction for attenuation was carried out on the displacement spectrum to obtain correct source parameters. The attenuation values used in the correction were k = 0.02 (Singh et al., 1990) and Q (f) = $98f^{0.72}$ (Singh et al., 2007); the first value correspond to the contribution on near surface attenuation and the second value to the attenuation along the path. The attenuation values are the best choice to represent the MVB zone, since the Q value was estimated based on records within the MVB and the k value based on records near the MVB zone, with seismic sources located at the subduction zone. At present, no detailed study has been carried out of attenuation solely based with shallow earthquakes within the MVB. However, for this type of study (short distance and high frequencies) the path attenuation has a lesser effect in the spectral decay than the near surface attenuation since this is what dominates the spectral decay, and which affects the most the evaluation of the correct corner frequency (f_o) (Fig. 6). In Figure 6 the shape of the theoretical source spectra was plotted for the displacement, according to the Brune (1970) model, thus allowing the identification of the correct spectral flat level (Ωo). In addition, a plot from the spectra of background noise signals was made to compare with the spectra of the seismic signal. The signal/noise ratio observed in Figure 6 (>> 1) allows for an adequate estimation of the correct f_o.

The results of spectral analysis are shown in Table 5. The first analysis was done based on a window of the corrected P wave displacement spectrum (Fig. 6a), where f_o = 6.0 Hz and Ωo =

3.03 x 10^{-6} m s, and consequently, values of a = 0.516 km, $\Delta\sigma$ = 5.1 bar and Mw = 3.4 were calculated. The result of Mw obtained through the inversion procedure and that from the spectral analysis were similar, being Mw = 3.5 and Mw = 3.4, respectively. Hence, the source area of the largest event was estimated to have a radius of 0.516 km. In contrast, an analogous second analysis using the S wave displacement (Fig. 6b) gave an estimate of Mw=2.9. We infer that this is because the S-wave spectral flat level was not as clearly identified as that of the P-wave, in particular at low frequencies (f < 2 Hz) (Fig. 6b).

3 Discussion

3.1 Relation with regional tectonics

A statistical analysis of the σ_1 and σ_3 stress axes (the maximum and minimum principal compressive stress axes, respectively) by means of rose histograms (Table 6 and Fig. 7), and taking into account all the focal mechanisms (shown in Fig. 3a), is in agreement with an azimuthal direction of the minimum compressive horizontal stress, σ_3, of approximately 260° (Fig. 7c). The lineaments of the geomorphological features, when compared to the focal mechanism results (Fig. 3a), also provide support for the notion that the fault associated to the largest shock has a strike of 174°, dip of 77° and rake of -85°. This fault and the average minimum compressive stress direction are consistent with the main trend of the southern extension of the BR province (Henry and Aranda-Gómez, 1992) much like the Sanfandila sequence of 1998 (Zúñiga et al., 2003) farther to the south. Thus, the results for the PES are yet additional evidence supporting the notion that the state of stress in this region is similar to that of the southern BR and may be even part of the same province.

3.2 Seismic risk and hazard

The frequency of occurrence of large shallow earthquakes in the MVB zone is much lower than that of the subduction zone. In Table 7 two earthquake catalogs are shown; the first is a list of 40 earthquakes (Mw between 5.0-8.0) used recently to estimate an attenuation relation by Arroyo et al. (2010) for the subduction zone and the second is a compilation of the historical seismicity in MVB (Ms between 4 - 7.8) as reported by Suter et al. (1996) and Zúñiga et al. (2003).

The low density of seismic instrumentation in the MVB (most of the stations are south of the MVB) has not allowed a study of this type on the shallow seismicity. For example, at this moment it is not

yet known: 1) what is the behavior of seismic attenuation from large shallow earthquakes within MVB, 2) what is the ground amplification level at different sites within the MVB, and 3) which buildings would be more affected by shaking, among others questions. These are some questions that must be answered with help of analysis such as the one presented here. Also, it is necessary to remember that the population is growing in this area at the fastest rate in Mexico.

For the MVB zone, due to the short source distance of urban centers to the possible causative faults, the risk posed by shallow local earthquakes may be larger than the risk due to the subduction earthquakes. The PGA amplitudes and their hypocentral distances (R_h) from this study are presented in Fig. 8 and Table 8. In Table 8 we can see that the PGA on the Extoraz community site, where the EXT1 station was located, was close to 100 cm s^{-2} at around R_h = 6.0 km, due to the largest earthquake from PES of Mw=3.5. On the other hand, the PGA amplitudes within the MVB zone due to subduction earthquakes can be estimated through an attenuation relation reported by Clemente-Chavez et al. (2012) based on records within the MVB. For example, this attenuation relation estimates a PGA of 1.38 cm s^{-2} for an earthquake of Mw=7.1 to a hypocentral distance of 523 km and a depth of 5 km (information of the event occurred on March 20, 2012 of Mw = 7.1, this is for a path between MVB sites and subduction events). Recently, this estimation was consistent with the observed subduction earthquake in Oaxaca that showed a maximum PGA of 1.3 cm s^{-2} recorded in Queretaro). Regarding the site amplification level observed in the PES, if the horizontal PGA is contrasted with the PGA from vertical component shown in the Fig. 5, in general it can be estimated that there is a site amplification of around 4 times in the horizontal ground motion with respect to the vertical. Finally, in Fig. 6 we see that the frequency range with the highest amplitudes, 0.5 – 6.0 Hz; is the range which can affect buildings of up to 20 levels, mainly. These different scenarios show, in principle (because at present, there is not enough data to contrast), the higher risk due to the shallow earthquakes within the MVB zone than those of the subduction zone (except for Mexico City which is a well known special case).

Another aspect observed in one of the seismic records was the existence of premonitory earthquakes for event No. 2 of Table 8 (Fig. 9). These earthquakes occurred 20 to 60 seconds before the main shock. When these premonitory earthquakes take place, they can be observed at short distances due to high signal/noise ratio. The importance of these earthquakes is the possibility of establishing an early warning for this region.

4 Conclusions

A sequence of small earthquakes occurred at the end of 2010 and beginning of 2011, near the town of Peñamiller, Queretaro, which is located at the northeast border of the seismogenic

zone known as the MVB. In the MVB zone the seismic activity is not too frequent, but there are precedents of large earthquakes occurring there (e.g. Suter et al., 1996). From the study of the 2010-2011 Peñamiller Earthquake Sequence, several important aspects were found:

1) The seismic location and source parameters were estimated through an inversion process and spectral analysis, whereby the largest earthquake had a moment magnitude of Mw = 3.5, that corresponds to a source area with a radius of 0.5 km, with a normal fault of strike of 174°, dip of 77° and rake of -85°. This earthquake occurred on February 8, 2011 at 19:53:48.6 UTC at latitude 21.039° and longitude -99.752° and at a 5.6 km depth. This location is 7 km southeast from downtown Peñamiller, and at 3 km from the Extoraz community.

2) In general, all the earthquake recordings correspond to normal faults. This, the lineaments of the geomorphological features, and the results of the statistical analysis of the σ_1 and σ_3 stress axes are congruent with the extensional regimen with east-west direction in agreement to that of the southern extension of the BR province. Furthermore, it is not far from the location of the largest historical event known to have occurred in the region (Nov 17, 1887, mb ~ 5.3) which Suter et al. (1996) attribute to the same stress province.

3) Twenty-four good quality acceleration seismic records were registered by a temporary seismic network from the UAQ. Six records correspond to epicentral distances less than 3.0 km, which are close to the seismic source of the largest event. With good quality records it is possible to see the P direct phase and to estimate the *k* attenuation value, among other things.

4) Most of the earthquakes discussed here have acceleration levels (up to 100 cm s^{-2} of PGA) greater that the largest acceleration values observed for subduction earthquakes in the north MVB area. This situation establishes the necessity of further study of shallow earthquakes in central Mexico, since the hazard and risk posed by this type of events is very much neglected at this time.

Finally, this paper has presented seismic information, which helps to gain more insight into the tectonic situation of the central Mexico region.

Acknowledgements

The authors are grateful to CONACYT for its support in this research. Alejandro Clemente Chavez wants to thank: CONACYT-Mexico for this funded support for his Ph-d studies under

the project number 227579; to Dr. Gilberto Herrera Ruíz and Dr. Aurelio Domínguez González for their funded support in the installation of the temporary seismic network and its monitoring; finally, to my students Ing. Edgardo Rocha Ugalde and Ing. José Luis Plancarte Escobar for their collaboration in the field works.

References

Aguirre-Díaz, G. J., Nieto-Obregón, J., and Zúñiga, F. R.: Seismogenic basin and range and intra-arc normal faulting in the central Mexican Volcanic Belt, Querétaro, México, Geol. J., 40, 215–243, doi: 10.1002/gj.1004, 2005.

Alaniz-Álvarez, S. A. and Nieto-Samaniego, A. F.: El sistema de fallas Taxco-San Miguel de Allende y la Faja Volcánica Transmexicana, dos fronteras tectónicas del centro de México activas durante el Cenozoico, Boletín de la Sociedad Geológica Mexicana, 57 (1), 63-80, 2005.

Alaniz-Álvarez, S. A., Nieto-Samaniego, A. F., and Ferrari, L.: Effect of the strain rate in the distribution of monogenetic and polygenetic volcanism in the Trans-Mexican volcanic belt, Geology, 26, 591-594, 1998.

Arroyo, D., García D., Ordaz, M., Mora, M. A., and Singh, S. K.: Strong ground-motion relations for Mexican interplate earthquakes, Journal of Seismology, 14, 769-785, 2010.

Bouchon, M.: A simple method for calculating Green's functions for elastic layered media, Bull. Seism. Soc. Am., 71, 959-972, 1981.

Brune, J. N.: Tectonic stress and the spectra of seismic shear waves from earthquakes, J. Geophys. Res., 75, 4997-5009, 1970.

Clemente-Chavez, A., Arroyo, G., Moisés, Zúñiga Ramón, Figueroa Ángel, Pérez Miguel A., and López Carlos S.: Relación de atenuación del movimiento del suelo para la aceleración máxima (PGA) sobre el Cinturón Volcánico Mexicano (MVB); análisis por trayectoria: Guerrero-Querétaro, Revista de Ingeniería Sísmica, 87, 67-93, 2012.

Del Gaudio, V., .Pierri, P., and Calcagnile, G.: Seismogenic zonation and seismic hazard estimates in a Southern Italy area (Northern Apulia) characterised by moderate seismicity rates, Nat. Hazards Earth Syst. Sci., 9, 161–174, 2009.

Demant, A.: Características del Eje Neovolcánico Transmexicano y sus problemas de interpretación, Revista Instituto de Geología, Universidad Nacional Autónoma de México, 2, 172-187, 1978.

Demant, A.: Interpretación geodinámica del volcanismo del Eje Neovolcánico Transmexicano, Revista Instituto de Geología, Universidad Nacional Autónoma de México, 5, 217-222, 1981.

Ferrari, L., López-Martínez, M., González-Cervantes, N., Jacobo-Albarrán, J. and Hernández-Bernal, M.S.: Volcanic record and age of formation of the Mexico City basin, Unión Geofísica Mexicana, Resúmenes GEOS, 23(2), 120, ISSN 0186-1891, 2003.

Fuentes, C.: Inversión de la estructura cortical del sur de México utilizando velocidades de fase y grupo de ondas superficiales, Master Thesis, Instituto de Geofísica, UNAM, 1997.

García-Palomo, A., Macías, J., and Garduño, V.: Miocene to recent structural evolution of the Nevado de Toluca volcano region, Central Mexico, Tectonophysics, 318, 281-302, 2000.

Gómez-Tuena, A., Orozco-Esquivel, T., y Ferrari, L.: Petrogénesis ígnea de la faja volcánica transmexicana, Boletín de la Sociedad Geológica Mexicana, Vol. Conmemorativo del Centenario, Temas selectos de la Geología Mexicana, Tomo LVII, no. 3, 227-285, 2005.

Havskov, J. and Ottemoller, L.: SEISAN: The earthquake analysis software, Institute of Solid Earth Physics, Norway, 2000.

Henry, C. D. and Aranda-Gómez, J. J.: The real southern Basin and Range: Mid- to Late cenozoic extension in Mexico, Geology, 20, 701-704, 1992.

Johnson, C. A. and Harrison, C. G. A.: Neotectonics in central Mexico, Phys. Earth Inter., 64, 187-210, 1990.

Kikuchi, M. and Kanamori, H.: Inversion of complex body waves - III: Bull. Seism. Soc. Am., 81, 2335-2350, 1991.

Martínez-Reyes, J. and Nieto-Samaniego, A. F.: Efectos geológicos de la tectónica reciente en la parte central de México, Revista Instituto de Geología, Universidad Nacional Autónoma de México, 9, 33-50, 1990.

Nieto-Samaniego, A. F., Ferrari, L., Alaniz-Alvarez, S. A., Labarthe-Hernández, G., and Rosas-Elguera, J.: Variation of Cenozoic extension and volcanism across the southern Sierra Madre Occidental Volcanic Province, Mexico, Geol. Soc. Am. Bull., 111, 347-363, 1999.

Nixon, G. T., Demant, A., Armstrong, R. L., and Harakal, J. E.: K-Arand geologic data bearing on the age and evolution of the Trans-Mexican Volcanic Belt, Geofís. Int., 26, 109-158, 1987.

Pasquaré, G., Ferrari, L., Perazzoli, V., Tiberi, M., and Turchetti, F.: Morphological and structural analysis of the central sector of the Transmexican Volcanic Belt, Geofís. Int., 26, 177-194, 1987.

Pasquaré, G., Garduño, V., Tibaldi, A., and Ferrari, M.: Stress pattern evolution in the central sector of the Mexican Volcanic Belt, Tectonophysics, 146, 353-364, 1988.

Polonia, A., Torelli, L., Gasperini, L., and Mussoni, P.: Active faults and historical earthquakes in the Messina Straits area (Ionian Sea), Nat. Hazards Earth Syst. Sci., 12, 2311–2328, doi:10.5194/nhess-12-2311-2012, 2012.

Rosas-Elguera, J. and Urrutia-Fucugauchi, J.: Tectonic control on the volcano-sedimentary sequence of the Chapala graben, western Mexico, International Geology Review, 40, 350 - 362, 1998.

Singh, S. K., Rodríguez, M., and Espindola J. M.: A catalog of shallow earthquakes of Mexico from 1900 to 1981, Bull. Seism. Soc. Am., 74, 267-279, 1984.

Singh, S.K., Mena, E., Anderson, J.G., Quaas, R., and Lermo, J.: Source spectra and RMS accelerarion of Mexican Subduction zone earthquakes, PAGEOPH, 133, 477-474, 1990.

Singh, S. K., Iglesias, A., García, D., Pacheco, J. F., and Ordaz, M.: Q of Lg waves in the Central Mexican Volcanic Belt, Bull. Seism. Soc. Am., 97, 1259-1266, 2007.

Sokos, E. N. and Zahradnik, J.: ISOLA a Fortran code and a Matlab GUI to perform multiple-point source inversion of seismic data, Computers & Geosciences, ISSN 0098-3004, doi: 10.1016/j.cageo.2007.07.005, 8, 34, 967-977, 2008.

Suter, M.: State of stress and active deformation in Mexico and western Central America in Decade of North American Geology, Neotectonics of North America edited by D. B. Slemmons, E. R. Engdahl, M. D. Zoback, and D. D. Blackwell, Geol. Soc. of Am., Boulder, Colorado, Decade Map, 1, 401-421, 1991.

Suter, M., Carrillo, M., López, M., and Farrar, E.: The Aljibes halfgraben - active extension in the transition zone between the trans-Mexican volcanic belt and the southern Basin and Range, Mexico, Geol. Soc. Am. Bull., 107, 627-641, 1995.

Suter, M., Carrillo-Martínez, M., and Quintero-Legorreta, O.: Macroseismic study of shallow earthquakes in the central and eastern parts of the Trans-Mexican volcanic belt, Bull. Seism. Soc. Am., 86, 1952-1963, 1996.

Suter, M., López-Martínez, M., Quintero-Legorreta, O., and Carrillo-Martínez, M.: Quaternary intra-arc extension in the central Trans-Mexican volcanic belt, Geol. Soc. Am. Bull., 113, 693-703, 2001.

Urrutia-Fucugauchi, J. and Rosas-Elguera, J.: Paleomagnetic study of the eastern sector of 21 Chapala Lake and implications for the tectonics of west-central Mexico, Tectonophysics, 239, 22 61-71, 1994.

Vipin, K. S., Anbazhagan, P., and Sitharam T. G.: Estimation of peak ground acceleration and spectral acceleration for South India with local site effects: probabilistic approach, Nat. Hazards Earth Syst. Sci., 9, 865–878, 2009.

Zúñiga, F. R., Pacheco, J. F., Guzmán-Speziale, M., Aguirre-Díaz, G. J., Espíndola, V. H., and Nava, E.: The Sanfandila earthquake sequence of 1998, Queretaro, Mexico: activation of an undocumented fault in the northern edge of central Trans-Mexican Volcanic Belt, Tectonophysics, 361, 229-238, 2003.

Table 1. a) Events analyzed in this study: Peñamiller Earthquake Sequence (PES); b) Station location .

a)

Event No.	UTC Date (yyyy/mm/dd)	Number Records	Station Name
1	2011/01/30	3	EXT1, PIL1, HIG1
2	2011/01/30	3	EXT1, PIL1, HIG1
3	2011/02/07	3	EXT1, PIL1, HIG1
4	2011/02/07	3	EXT1, PIL1, HIG1
5	2011/02/08	3	EXT1, PIL1, HIG1
6	2011/03/01	3	EXT1, PIL1, HIG2
7	2011/03/01	3	EXT1, PIL1, HIG2
8	2011/03/26	3	EXT1, PEN2, HIG2
		24	

b)

Station Name	Location		
	Community	Lat. (°N)	Long. (°W)
EXT1	Extoraz	21.036	-99.777
PIL1	Pilon	21.065	-99.775
HIG1	Higuerillas	20.920	-99.763
PEN2	Peñamiller Center	21.054	-99.814
HIG2	Higuerillas	20.921	-99.770

Table 2. Velocity structure used in the location and inversion procedures.

Depth (km)	Vp (km/s)	Vs (km/s)
0.0	4.15	2.40
2.2	5.06	2.92
5.2	6.10	3.52
7.0	6.29	3.63
20.3	7.45	4.30
99.0	8.04	4.64

Table 3. Results of the locations of all events analyzed: Peñamiller Earthquake Sequence (PES).

		Origin time	Location			Error			rms
Event No.	UTC Date (yyyy/mm/dd)	UTC Hour (hh:mm:ss)	Lat. (°)	Long. (°)	H (km)	Lat. (km)	Long. (km)	H (km)	(s)
1	2011/01/30	17:54:22.50	21.034	-99.756	5.7	0.3	1.5	0	0.08
2	2011/01/30	17:54:41.70	21.034	-99.756	5.6	0.3	1.5	0	0.08
3	2011/02/07	00:16:34.00	21.039	-99.754	5.5	0.3	1.2	0	0.07
4	2011/02/07	09:42:54.50	21.024	-99.725	2.0	0.6	1.6	2.0	0.08
5	2011/02/08	19:53:48.60	21.039	-99.752	5.6	1.2	0.3	0	0.06
6	2011/03/01	12:59:40.70	21.031	-99.759	6.1	0.3	2.1	0	0.09
7	2011/03/01	13:11:28.10	21.033	-99.758	6.1	0.3	1.7	0	0.06
8	2011/03/26	01:42:17.40	21.015	-99.806	4.3	0.5	0.8	1.5	0.03

				Averages	5.11	0.48	1.34	0.44		0.07

Table 4. Earthquake source parameters of best fit solutions from the Peñamiller sequence.

Event No.	UTC Date (yyyy/mm/dd)	Origin time UTC Hour (hh:mm:ss)	Location Lat. (°N)	Long. (°W)	H (km)	Magnitude Mw	Strike ϕ (°)	Dip δ (°)	Rake λ (°)	Number Records
1	2011/01/30	17:54:22.50	21.034	-99.756	5.7	2.1	154	61	-116	3
2	2011/01/30	17:54:41.70	21.034	-99.756	5.6	3.0	108	45	-149	3
3	2011/02/07	00:16:34.00	21.039	-99.754	5.5	2.9	41	57	-162	3
4	2011/02/07	09:42:54.50	21.024	-99.725	2.0	2.5	268	86	-5	3
5	2011/02/08	19:53:48.60	21.039	-99.752	5.6	3.5	174	77	-85	3
6	2011/03/01	12:59:40.70	21.031	-99.759	6.1	3.2	85	67	-152	3
7	2011/03/01	13:11:28.10	21.033	-99.758	6.1	2.7	133	64	-143	3
8	2011/03/26	01:42:17.40	21.015	-99.806	4.3	2.9	124	34	-14	3

Table 5. Results of spectral parameters from the largest earthquake in Peñamiller which occurred on 2011/02/08 at 19:53:48.60 UTC.

Phase	Ωo (m s)	fo (Hz)	a (m)	Δσ (bar)	Mo (N m)	Mw
P	3.03E-06	6.0	516	5.1	1.59E+14	3.4
S	3.63E-06	5.8	228	11.1	3.02E+13	2.9

Ωo=spectral flat level, fo=corner frequency, a=source radius, $\Delta\sigma$ =static stress drop, Mo=seismic moment and Mw=magnitude moment.

Table 6. Earthquake source parameters and values of the maximum (σ_1) and minimum (σ_3) compressive principal stresses axes from the PES.

Event No.	UTC Date (yyyy/mm/dd)	Time origin UTC Hour (hh:mm:ss)	Magnitude Mw	Strike ϕ (°)	Dip δ (°)	Rake λ (°)	σ_1 (P) Azimuth (°)	σ_1 (P) Plunge (°)	σ_3 (T) Azimuth (°)	σ_3 (T) Plunge (°)
1	2011/01/30	17:54:22.50	2.1	154	61	-116	19	63	263	13
2	2011/01/30	17:54:41.70	3.0	108	45	-149	310	50	57	15
3	2011/02/07	00:16:34.00	2.9	41	57	-162	257	35	355	12
4	2011/02/07	09:42:54.50	2.5	268	86	-5	223	7	313	2
5	2011/02/08	19:53:48.60	3.5	174	77	-85	90	58	261	32
6	2011/03/01	12:59:40.70	3.2	85	67	-152	305	35	214	2
7	2011/03/01	13:11:28.10	2.7	133	64	-143	352	44	257	5
8	2011/03/26	01:42:17.40	2.9	124	34	-14	104	44	343	29

Table 7. Larger earthquake catalogs of the two seismogenic zones in contrast.

Subduction (SUB2 and SUB3)

Event No.	UTC Date (yyyy/mm/dd)	Location Lat. (°N)	Long. (°W)	H (km)	Magnitude Mw
1	1985/09/19	18.14	-102.71	17.0	8.0
2	1985/09/21	17.62	-101.82	22.0	7.6
3	1988/02/08	17.45	-101.19	22.0	5.8
4	1989/03/10	17.45	-101.19	20.0	5.4
5	1989/04/25	16.61	-99.43	16.0	6.9
6	1989/05/02	16.68	-99.41	15.0	5.5
7	1990/01/13	16.82	-99.64	16.0	5.3
8	1990/05/11	17.12	-100.87	21.0	5.5
9	1990/05/31	17.12	-100.88	18.0	5.9
10	1993/05/15	16.47	-98.72	16.0	5.5
11	1993/10/24	16.65	-98.87	26.0	6.6
12	1995/09/14	16.48	-98.76	16.0	7.3
13	1996/03/13	16.59	-99.12	25.0	5.1
14	1996/03/27	16.36	-98.30	18.0	5.4
15	1996/07/15	17.33	-101.21	27.0	6.6
16	1996/07/18	17.44	-101.21	25.0	5.4
17	1997/01/21	16.42	-98.21	28.0	5.4
18	1997/12/16	16.04	-99.41	27.0	5.9
19	1998/05/09	17.5	-101.24	23.0	5.1
20	1998/05/16	17.27	-101.34	28.0	5.1
21	1998/07/05	16.81	-100.14	25.0	5.3
22	1998/07/11	17.35	-101.41	29.0	5.4
23	1998/07/12	16.85	-100.47	26.0	5.5
24	2001/09/04	16.29	-98.37	20.0	5.5
25	2001/11/10	16.09	-98.32	17.0	5.4
26	2002/06/07	15.99	-96.92	20.0	5.9
27	2002/06/07	15.96	-96.93	19.0	5.5
28	2002/06/19	16.29	-98.02	20.0	5.5
29	2002/08/05	15.94	-96.26	15.0	5.4
30	2002/08/27	16.16	-97.54	15.0	5.6
31	2002/08/30	16.76	-100.95	15.0	5.2
32	2002/09/25	16.80	-100.12	12.0	5.7
33	2002/11/08	16.28	-98.12	16.0	5.8
34	2002/12/10	17.36	-101.25	24.0	5.4
35	2003/01/10	17.01	-100.35	28.0	5.1
36	2003/01/22	18.62	-104.12	10.0	5.2
37	2004/01/01	17.27	-101.54	17.0	6.0
38	2004/01/01	17.32	-101.47	27.0	5.5
39	2004/02/06	18.16	-102.83	12.0	5.6
40	2004/06/14	16.19	-98.13	20.0	5.9

Information reported by Arroyo et al. (2010).

MVB

Event No.	UTC Date (yyyy/mm/dd)	Location Town, State	Location Lat. (°N)	Long. (°W)	H (km)	Magnitude Mw/m_b Ms
1**	1568/12/27	Jalisco	≈ 20.1	≈ -103.6		7.5-7.8 / -
2**	1875/12/27	Near Guadalajara	≈ 21	≈ -103.9		7.1 / -
3*	1887/11/26	Pinal, Queretaro	21.14	-99.63	-	- / 5.3
5*	1912/11/19	Acambay, Mexico	19.83	-99.92	5-15	7.0** / 6.9
6*	1920/01/04	Jalapa, Veracruz	19.27	-99.08	15.0	- / 6.5
7*	1950/03/11	Ixmiquilpan, Hidalgo	20.35	-98.97	-	- /4.9
8 +	1935/06/29	Michoacan	18.75	-103.50	-	6.9
9*	1976/03/25	Cardonal, Hidalgo	20.62	-99.09	15.0	- /5.3
10*	1979/02/22	Maravatio, Michoacan	19.89	-100.18	8±3	- /5.3
11*	1987/01/27	Actopan, Hidalgo	20.31	-99.21	15.0	- /4.1
12*	1989/09/10	Landa, Queretaro	21.04	-99.43	10.0	- /4.6

* Information reported by Suter et al.(1996); **Information reported by Zúñiga et al.(2003); + Information reported by Singh et al. (1984).

Table 8. Amplitude of peak ground acceleration with respect to hypocentral distance from all events in each station.

	Event No.[Mw]							
	1 [2.1]	2 [3.0]	3 [2.9]	4 [2.5]	5 [3.5]	6 [3.2]	7 [2.7]	8 [2.9]
	Peak Ground Acceleration, PGA (cm/s^2) / Hypocentral distance R_h (km)							
Station								
EXT1	4.66 / 6.11	27.23 / 6.02	9.28 / 6.01	8.26 / 5.93	93.63 / 6.19	36.24 / 6.41	7.82 / 6.42	8.12 / 5.74
PIL1	4.95 / 6.95	30.40 / 6.86	5.58 / 6.59	4.42 / 7.19	83.12 / 6.74	16.81 / 7.36	14.75 / 7.28	-
HIG1	0.69 / 13.92	1.91 / 13.88	0.50 / 14.36	0.52 / 12.39	3.44 / 14.41	-	-	-
HIG2	-	-	-	-	-	1.51 / 13.68	0.38 / 13.89	1.18 / 11.87
PEN2	-	-	-	-	-	-	-	4.91 / 6.14

PGA is root mean square of the horizontal components.

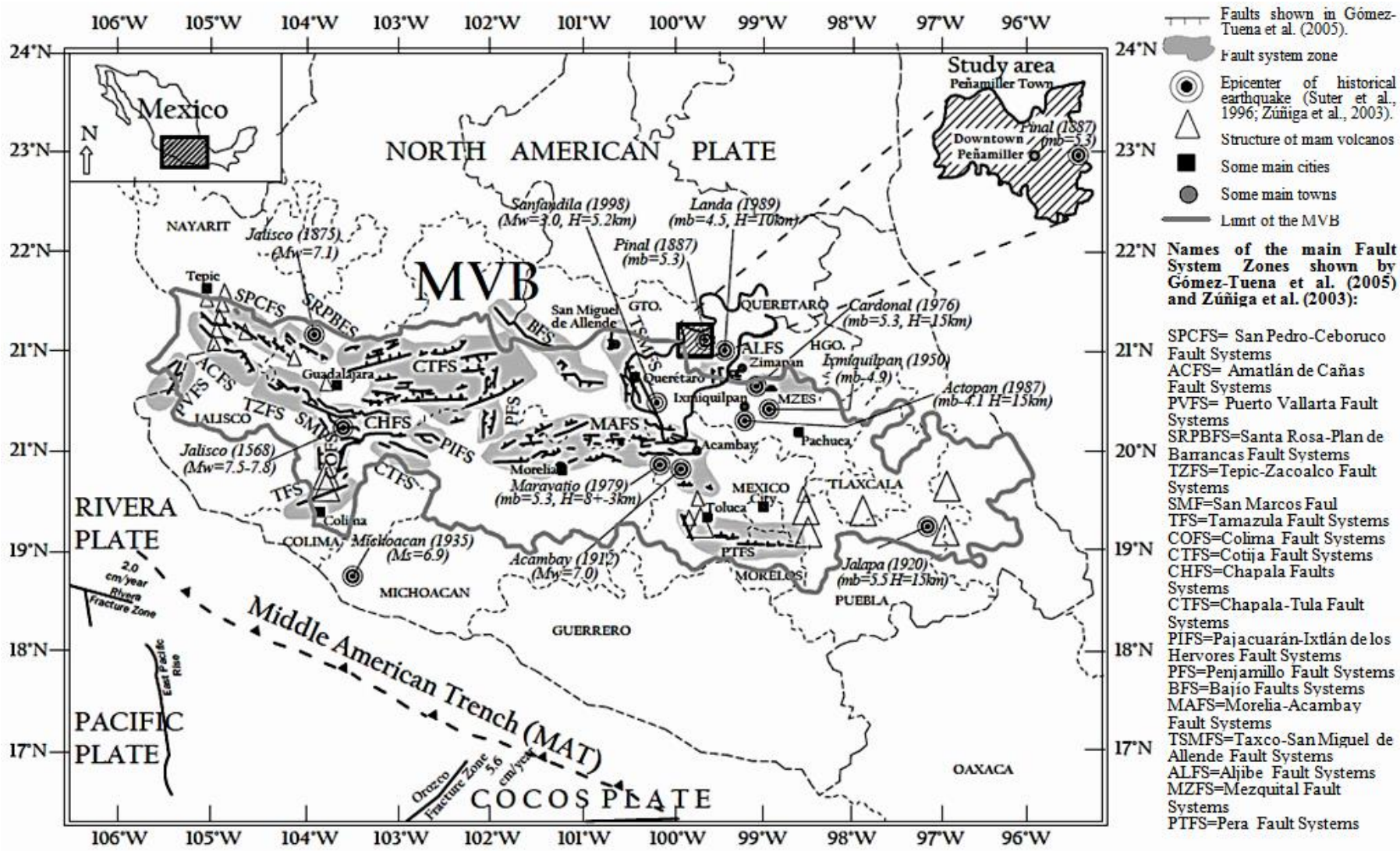

Figure 1. Regional tectonic situation, main faults systems zones, historical large earthquakes of the MVB and study area.

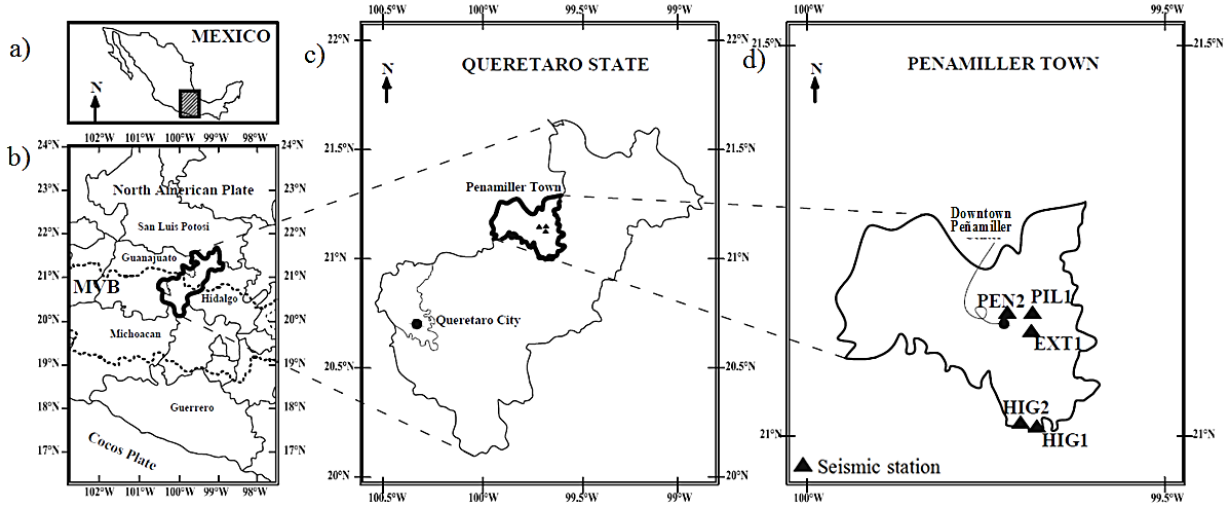

Figure 2. The study area: northeast edge of the MVB. Location and identification of: (a) Mexico, (b) Queretaro state within Mexico and delimitation of MVB zone with dotted line, (c) Peñamiller Town and Queretaro City within Queretaro state, and (d) Seismic stations and Downtown Peñamiller.

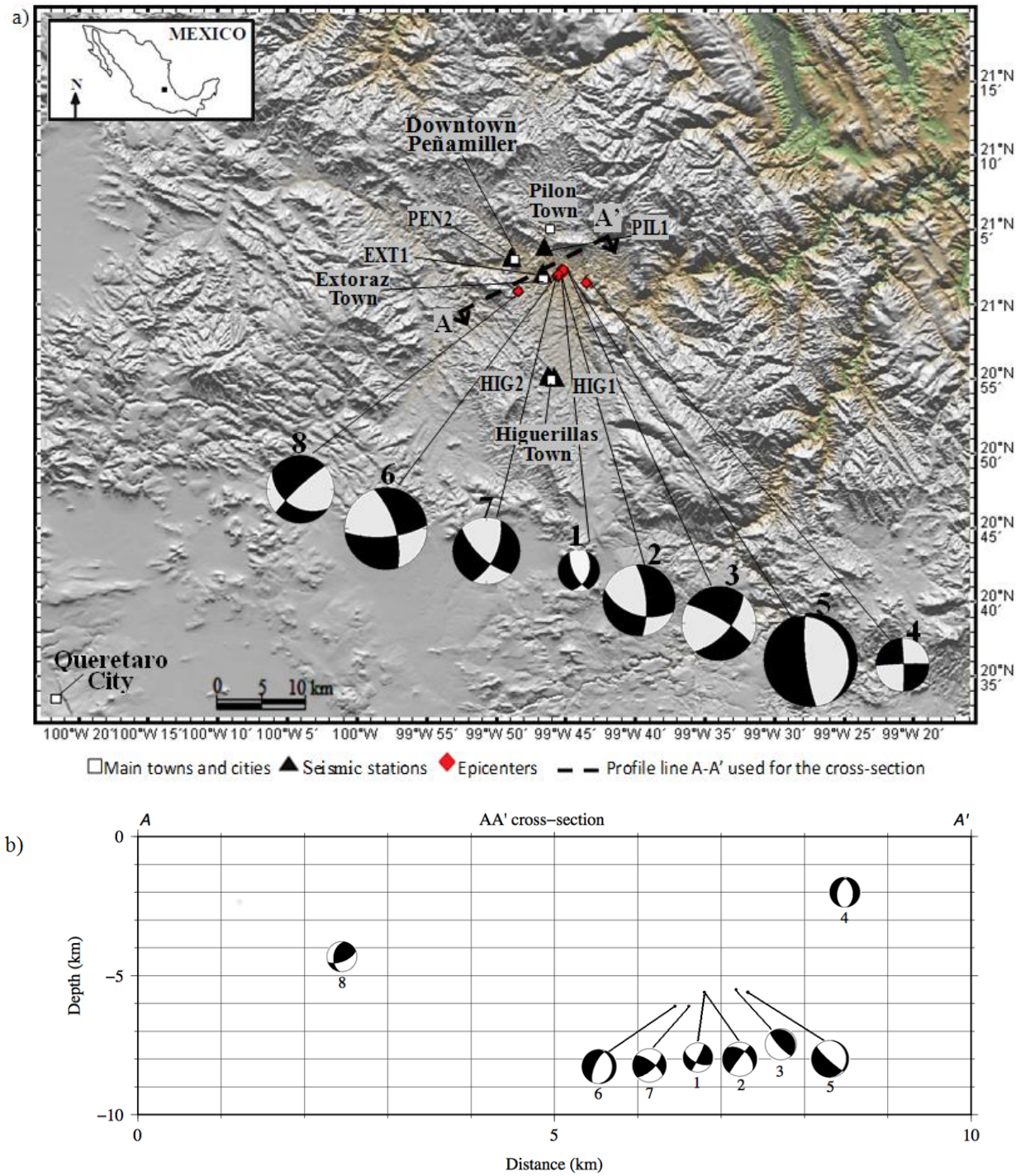

Figure 3. (a) Epicenters of the Peñamiller Earthquakes Sequence and fault plane solutions (Focal Mechanisms) for eight events employed in the inversion procedure. (b) Cross-section A-A' with hypocenters.

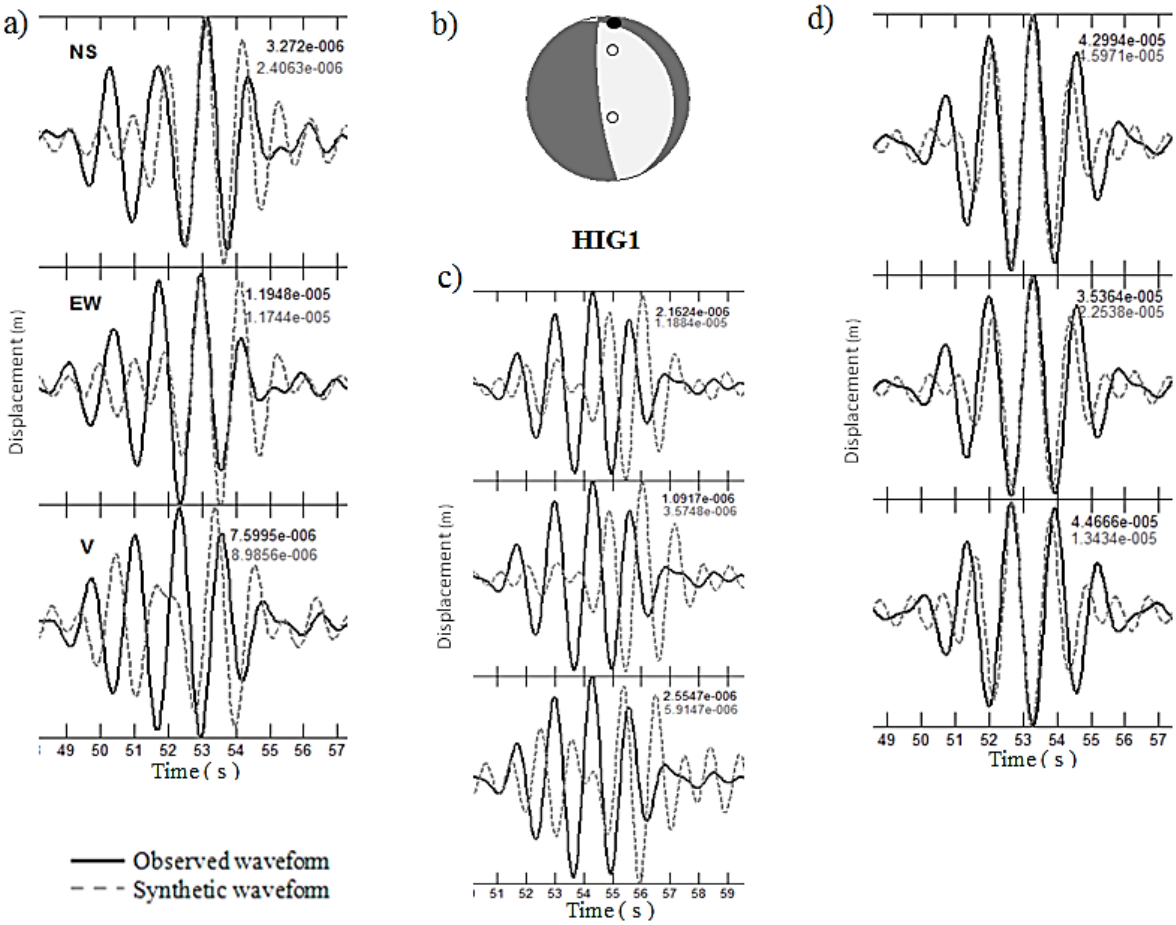

Figure 4. (a), (c) and (d) Observed and synthetic waveforms and their displacement amplitudes at each station for the largest earthquake Mw=3.5 occurred on February 8, 2011 at 19:53:48.6 UTC. (b) Focal mechanism; first motion polarities are shown to compare with the best solution.

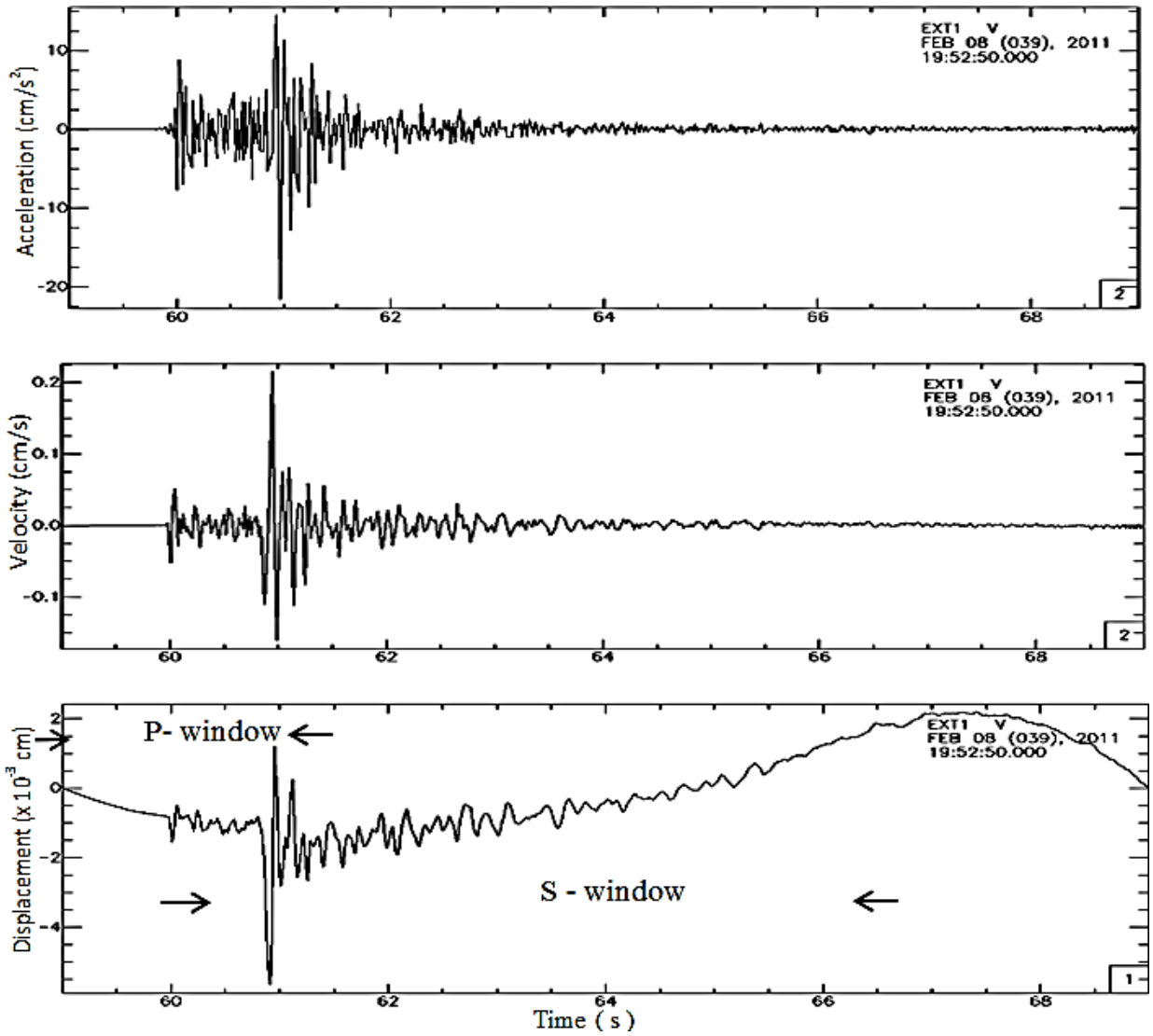

Figure 5. Acceleration, velocity and displacement signal from the largest earthquake in Peñamiller that occurred on 8 February 2011 at 19:53:48.60 UTC are shown. Long of each phase-window on displacement signal for the spectral analysis are indicated with arrows. Note: Although P-window includes some of the S phase, this is eliminated by the taper which diminishes the effects of the window extremes.

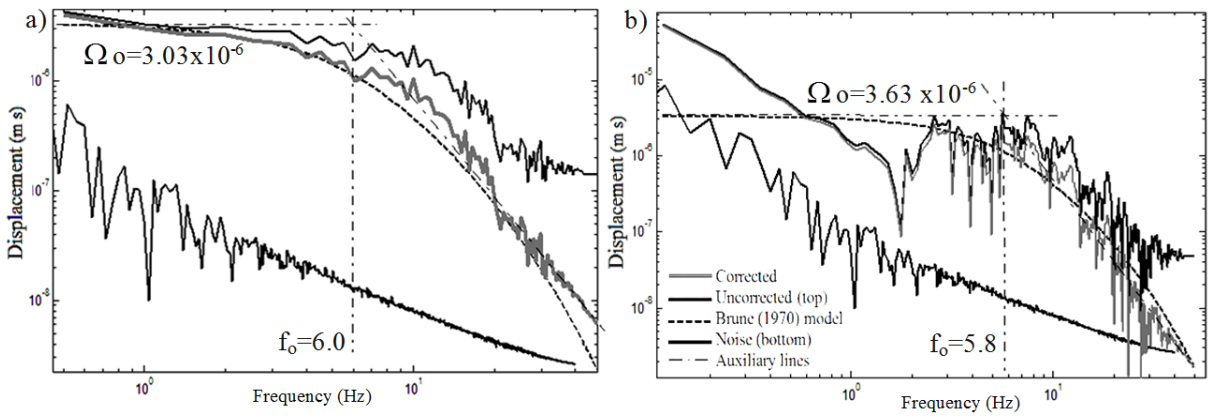

Figure 6. (a) P-wave and (b) S-wave displacement spectrums from the largest earthquake in Peñamiller corrected and uncorrected for attenuation are shown. Spectral shape according to the Brune (1970) model and noise spectrum are also shown. The corner frequency f_o and spectral flat level Ωo are identified.

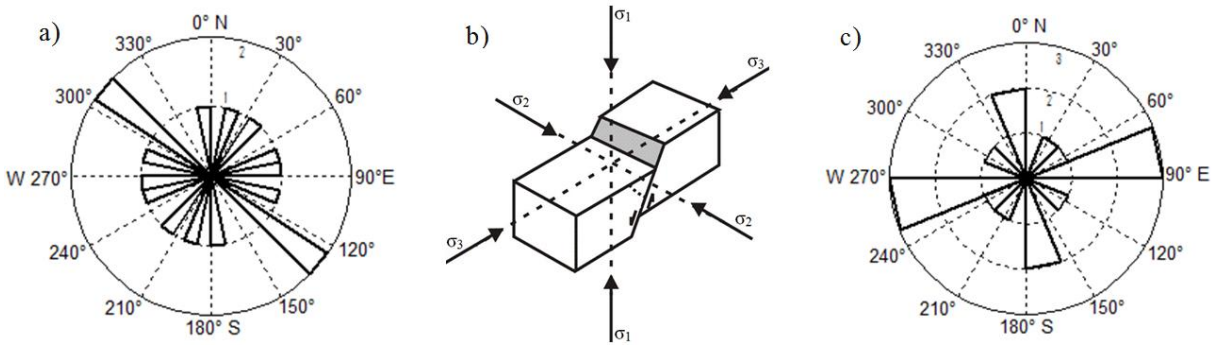

Figure 7. Rose histograms: a) Direction of maximum vertical (σ_1) and c) minimum horizontal compressive stresses axes (σ_3). b) A representation of the principal stress axes in a block-diagram of a normal fault.

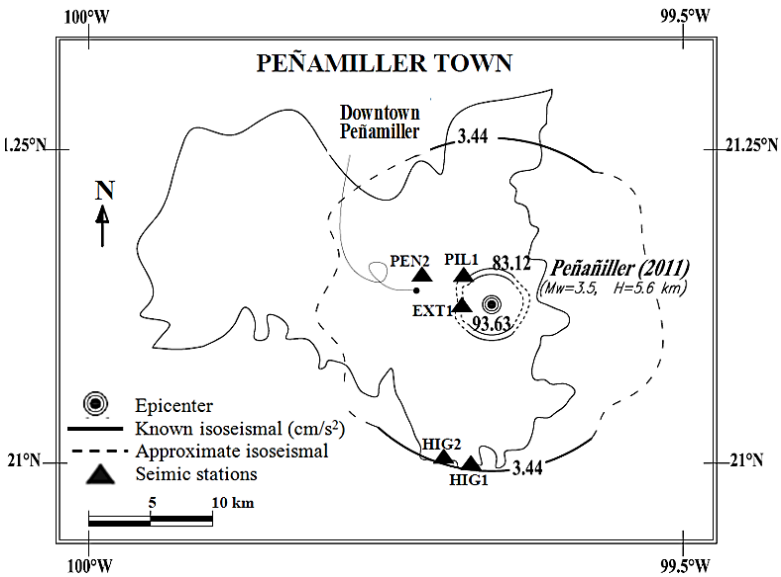

Figure 8. Isoseismal of PGA amplitudes for the largest earthquake of Mw=3.5, seismic stations and downtown Peñamiller are shown.

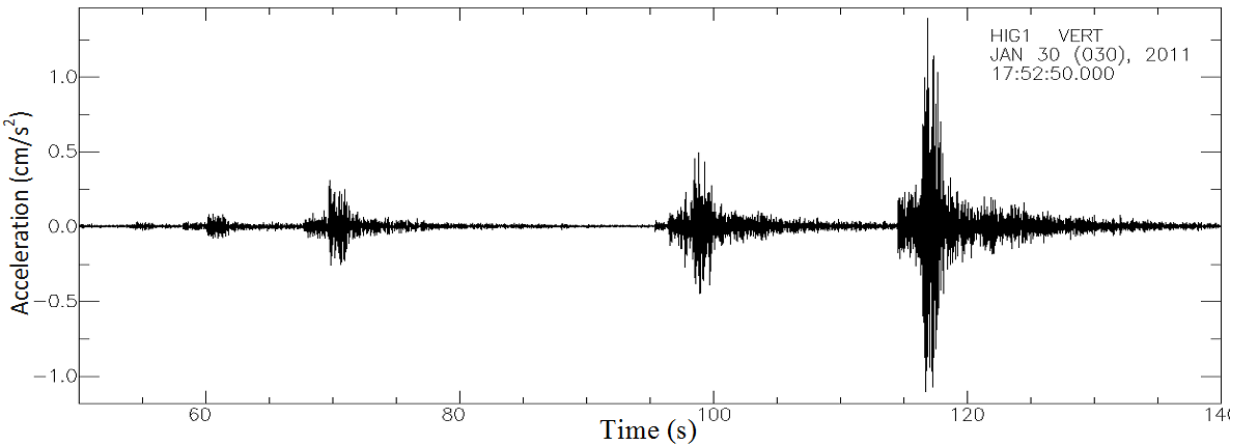

Figure 9. Premonitory earthquakes for the event No. 2 of Mw=3.0 are shown. In figure is observed that there are between 20 to 60 seconds before of the main shock.